Coseismic Deformation of the Indonesian Geospatial Reference System 2013 from the 2022 Cianjur Earthquake

Awaluddin, M.,[1*] Yuwono, B. D.,[1] Syetiawan, A.[2] and Fauziah, I.[1]
[1]Department of Geodetic Engineering, Diponegoro University, Indonesia
E-mail: awal210874@gmail.com,* ORCID ID: https://orcid.org/0000-0002-1644-068X
bambangdarmoyuwono@lecturer.undip.ac.id, imasfauziah@alumni.undip.ac.id
[2]National Research and Innovation Agency, Indonesia, E-mail: agungsyetiawan@gmail.com
Corresponding Author

DOI: https://doi.org/10.52939/ijg.v22i5.4985

Abstract
Indonesia is a country with high seismic activity. Since 2013, Indonesia has used a semi-dynamic geodetic datum, also known as a reference system. Earthquake events can cause surface deformation and alter the coordinates of the Indonesian Geospatial Reference System 2013 (SRGI 2013) points. Changes in these coordinates will affect the computation of new coordinates referenced to SRGI 2013. On November 21, 2022, an earthquake struck the Cianjur area of Indonesia. This study aims to calculate the displacement of SRGI 2013 points around the epicenter of the Cianjur Earthquake due to coseismic deformation using continuous GNSS observation data and to analyze the effect of this deformation on the SRGI 2013 reference frame. The earthquake caused significant horizontal displacement at STA CJUR and significant vertical displacement at five GNSS CORS SRGI 2013 stations. The horizontal displacement of the GNSS CORS stations ranges from 0.001 m to 0.0445 m (1 mm to 44.5 mm). The vertical displacement ranges from −0.0038 m to 0.0125 m (−3.8 mm to 12.5 mm). The largest horizontal and vertical displacements occurred at CJUR Station, which is the closest station to the epicenter. Although the horizontal deformation at STA CJUR only affects the 1:100 class 1 base map scale, it also affects control point measurement activities for mapping at a scale of 1:1,000 or smaller. Therefore, redefining the STA coordinates using new epochs or incorporating earthquake-induced deformation information into the deformation model is recommended. The densification of control points in Indonesia's SRGI reference framework will henceforth take into account locations near earthquake sources in order to support more accurate calculation of earthquake-induced deformation models. A more accurate deformation model can improve the quality of SRGI as a semi-dynamic datum.

Keywords: Coseismic, Cianjur, deformation, GNSS, SRGI 2013

1. Introduction

Indonesia is an archipelagic country located on active tectonic plates. Indonesia is a meeting point for three large tectonic plates: Indo-Australian, Eurasian, and Pacific. This condition makes Indonesia a country with many earthquake sources. According to data from the Meteorology, Climatology, and Geophysics Agency (BMKG), 11,660 earthquakes were recorded in 2019 [1]. The Geospatial Reference System is a national coordinate system that uses geodetic data. This coordinate system is consistent and compatible with the global coordinate system. Specifically, this reference system determines latitude, longitude, height, scale, gravity, and orientation covering the entire territory of Indonesia. In practice, this geospatial reference system is implemented as a Geodetic Control Network (JKG). Each geodetic control point in the JKG will have precise coordinate values, including horizontal, vertical, and gravity coordinates [2].

Indonesia's geodetic datum or reference system was first defined in the 19th century. The reference system was still a topocentric geodetic datum, locally static. The first national static topocentric datum was used in 1975. The datum was called Datum Indonesia 1974 (ID'74). After that, Indonesia used the National Geodetic Datum 1995 (DGN '95), a static geocentric datum realized using Global Positioning System (GPS) observations. DGN '95 was referred to as ITRF 2000, so it was a global datum. The datums used in Indonesia Local Datum, ID '74, and DGN '95

are static datums. The coordinate values of all control points in the reference frame are fixed and do not change as long as the datum is in use. These static datums were deemed no longer suitable for Indonesia's conditions, given that the country is located in an active tectonic area. Earthquake events and active plate movements cause surface deformation in and around Indonesia, resulting in changes to the coordinates of control points used as the geospatial reference framework. Therefore, the datum must account for deformation effects due to plate tectonic processes [2].

Semi-dynamic datum defines a set of coordinates from the Coordinate Framework Network control points, with each control point having one coordinate value set at a particular epoch reference (freeze coordinates). A semi-dynamic datum already accounts for plate tectonics in determining a position's coordinates because it includes a deformation model [3]. Since 2013, Indonesia has used a semi-dynamic geodetic datum or reference system. The new Geodetic Datum, the Indonesian Geospatial Reference System 2013 (SRGI 2013), is a global semi-dynamic datum bound to ITRF 2008. SRGI 2013 was defined on January 1, 2012, and equipped with a deformation model [3].

Survey measurement and mapping in Indonesia must be referenced to the SRGI 2013 datum. The coordinates of new points are calculated from the reference frame points in SRGI 2013, epoch 2012. Using deformation models equipped with GNSS CORS displacement velocity vectors, the coordinates of new points can be calculated for the desired epoch (BIG, 2024). Earthquake events can cause surface deformation and coordinate displacements of the SRGI 2013 points. The displacement of coordinates will affect the calculation of new coordinates that are referenced to SRGI 2013. Therefore, the calculation of the deformation effect is required if an earthquake occurs within the area covered by the SRGI 2013 reference frame points. A semi-dynamic datum is implemented to maintain the accuracy of the geodetic datum affected by deformation from seismic activity. The semi-dynamic datum consists of a static geodetic datum and a surface deformation model. The deformation model was created to accommodate the velocity calculations of reference frame points on the datum. Coseismic deformation due to earthquakes must also be calculated to update the reference frame and its deformation model [4].

The earthquake in the Palu area on September 28, 2018, with a magnitude of 7.4, was caused by the coseismic activity of the Palu Koro Fault [5]. Coseismic deformation calculated at five CORS GNSS stations ranged from 7.7852 mm to 477.130 mm. The magnitude of the deformation varies with the station's proximity to the epicenter, with the most significant displacement at the TOBP point and the least at CPRE [6]. This study calculated displacement only within the 2013 SRGI reference framework, before and after the earthquake. No analysis of the 2013 SRGI reference framework was performed. The Lombok earthquake with a magnitude of 6.4 occurred on July 29, 2018. The deformation calculation used the remote sensing method, SAR data from Sentinel-1A Satellite Imagery (Interferometric Wide Swath (IW)), and the DInSAR method. The deformation effect caused by the earthquake in Lombok, based on the DInSAR method, is -0.001 m to -0.134 m with an average of -0.026 m [7]. This study did not calculate the deformation at the 2013 CORS SRGI station.

The coseismic deformation caused by the Mentawai Earthquake on October 25, 2010, was calculated using GPS observation data from the Sumatran GPS Array (SuGAr) points. The earthquake measured 7.8 and triggered a tsunami. The maximum displacement of these points was 45 cm for the horizontal component and 7.8 cm for the vertical component. This study used GPS CORS deformation results to estimate the slip distribution on the earthquake plane [8]. Earthquake-induced deformation was calculated for five earthquakes that occurred in the Kyrgyz Republic, China, and Tajikistan between 2014 and 2017 using the Differential Interferometric Synthetic Aperture Radar (DInSAR) technique on Sentinel-1 data. A deformation of 28 mm was detected in two earthquakes with magnitudes >6. While in three other earthquakes with magnitudes greater than five and less than 6, no significant deformation was found [9]. A double earthquake struck Turkey on February 6, 2023. The first earthquake had a magnitude of 7.8, and the second 7.5. High-rate GNSS data were used to study the static and kinematic coseismic displacements and to invert the fault displacement distribution of the double earthquake. The maximum coseismic displacements for the first and second earthquakes were 0.38 m and 4.4 m, respectively. Kinematic displacements were also calculated to analyze the earthquake's faulting processes [10].

A study conducted in Uzbekistan investigated the potential of GNSS data for earthquake zoning and risk assessment in a seismically active region influenced by the interaction of several tectonic plates. Using GNSS velocities from two annual periods (2018–2019 and 2019–2020), combined with GIS and spline interpolation, the study identified high seismic risk across the entire study area, with rotational movements in the tectonic plate junction zone and movement rates ranging from 1.56 to 20.3 mm/year and 1.64 to 14 mm/year for the two

respective periods. The study concluded that GNSS analysis can provide valuable insights into seismic hazard assessment and improve understanding of tectonic processes leading to earthquakes. However, this study did not analyze deformations occurring within the geodetic datum of Uzbekistan [11]. On November 21, 2022, an earthquake struck the Cianjur area of Indonesia. The epicenter was at coordinates 6.836°S 106.997°E with a depth of 10 km. The earthquake's intensity reached VIII on the MMI scale, indicating severe shaking. Given this earthquake's intensity, it is estimated that the deformation in the area around the epicenter is quite significant geologically [12].

Around the Cianjur earthquake epicenter, eleven Continuously Operating Reference Stations (CORS) GNSS points of the SRGI 2013 reference frame, belonging to the Geospatial Information Agency (BIG), are located. The distance from the station to the epicenter varies to approximately 70 km. The eleven points are with the CJUR, CLDO, CUMI, BAKO, CLBG, CPWK, CPTU, CIAN, CTAN, CANG, and CBTU codes. Of the eleven points, it is estimated that three are affected by the earthquake shaking on the USGS Intensity Map scale V-VIII. The three points are CJUR, CLDO, and CUMI, less than 40 km from the epicenter [12]. This study aims to calculate the displacement of SRGI 2013 points around the epicenter of the Cianjur Earthquake due to coseismic deformation using continuous GNSS observation data. With the availability of GNSS data from 11 points around the epicenter, the displacements of 7 points CJUR, CLDO, CUMI, BAKO, CPWK, CBTU, and CLBG will be calculated based on the availability of RINEX data. The objectives of this study are consistent with those of deformation studies using GNSS data for the 2018 Palu earthquake, the 2010 Mentawai earthquake, and the 2023 Turkey earthquake. In addition, remote sensing satellite data were utilized for the 2018 Lombok earthquake and five earthquakes that occurred in the Kyrgyz Republic, China, and Tajikistan between 2014 and 2017 [5][6][7][8] and [9].

The purpose of studying crustal deformation is not only to map earthquake sources but also to examine geodetic datums, both dynamic and semi-dynamic. Therefore, this study also analyzes the effect of earthquake-induced deformation on the SRGI 2013 reference frame as a semi-dynamic datum. Will earthquake-induced deformation affect measurement and mapping activities that reference the SRGI 2013 reference frame? At what map scale will the displacement have a significant effect? Consequently, is it necessary to recalculate the coordinates of the reference frame points affected by earthquake-induced deformation?

2. Cianjur Earthquake 2022

The Cianjur Earthquake, centered at coordinates 6.8360 S, 106.9970 E, occurred on November 21, 2022, with a magnitude of 5.6. Based on information from the BMKG (Meteorology, Climatology, and Geophysics Agency), the earthquake occurred from November 21, the peak of the earthquake, until November 22, 2022. In addition to Cianjur Regency, the epicenter of the quake, several areas around Cianjur were affected, including Garut, Sukabumi, Lembang, Cimahi, Bandung City, Jakarta, Depok, Tangerang, and Bogor [13]. Three foreshocks preceded the main shock. Aftershocks indicated the presence of a pair of conjugate faults trending NNW-SSE (North Northwest-South Southeast), approximately 8 km long, and WSW-ENE (West Southwest – East Northeast), approximately 5 km long [14].

The main shock of the Cianjur Earthquake was felt in Cianjur City up to V-VI MMI (Modified Mercalli Intensity), IV-V MMI in Garut and Sukabumi, III MMI in Cimahi, Lembang, Bandung City, Cikalong Wetan, Rangkasbitung, Bogor, and Bayah, II-III MMI in South Tangerang, Jakarta, and Depok. High-rate GPS data were used to determine the ground velocity waveform with a post-processing method in the Cianjur Earthquake. The results showed that the horizontal velocity at the CJUR station was significant, whereas the vertical velocity was not. The maximum ground velocity reached up to 11.5 cm/s from the time of origin of the earthquake, the value of which correlated with the VI MMI scale [15].

The Cianjur Earthquake was triggered by underground movement along a fault. The fault identified in the Cianjur region is the Cimandiri fault. However, the earthquake's epicenter and the Cimandiri fault line are approximately 20 km apart. The Indonesian Meteorology, Climatology, and Geophysics Agency (BMKG) indicated that a new fault, the Cugenang Fault, was responsible for the earthquake. The main quake occurred in the WSW-ENE direction, with sinistral (left-lateral) movement [16]. The earthquake in Cianjur was a shallow crustal tectonic earthquake of the mainshock-aftershock type, namely a main earthquake followed by a series of aftershocks [17]. Deformation due to the Cianjur Earthquake was calculated using Remote Sensing technology with the InSAR method. The calculated deformation reached a maximum of +5.8 cm in the vertical direction in the Cugenang District, the earthquake's epicenter. In addition, the horizontal

deformation due to the aftershocks was quite large, reaching ±12 cm to the southeast [18].

Seismological analysis of 45 seismic stations and statistical analysis of mainshock and aftershock data in the Cianjur earthquake area were conducted using Sentinel-1 radar imagery and DInSAR. The study results showed land subsidence in the Cianjur area and its surroundings during the primary earthquake on November 21, 2022, with an average deformation of approximately -5 cm. In contrast, the deformation measured during the aftershocks showed land uplift, averaging 10 cm. Examining the deformation pattern in the 2022 Cianjur earthquake series revealed an increase in deformation around the Cugenang District, with an orientation from northwest to southeast [19].

3. Indonesia Continuously Operating Reference Station (Ina-CORS) and SRGI 2013

Indonesia Continuously Operating Reference Station (Ina-CORS) is an active geodetic control network in Indonesia comprising permanent Global Navigation Satellite System (GNSS) stations on the earth's surface, each equipped with a GNSS satellite signal recorder, antenna, and data communication system. According to the Head of BIG Regulation Number 13 of 2021, CORS is defined as a Geodetic Control Point where continuous position observations are carried out using geodetic-type GNSS receiver equipment. The station continuously receives GNSS satellite signals 24 hours a day and provides position correction services to users. In practice, Ina-CORS can be used for various purposes, both practical and scientific. Regarding practical needs, Ina-CORS can be used for surveying, mapping, and even precise navigation. Ina-CORS can provide real-time kinematic (RTK) position correction services for users who need instant position determination. In other cases that do not require instant positioning results, users can obtain positioning results through post-processing. Ina-CORS can be used to maintain the accuracy and precision of the geodetic basic framework, which supports the implementation of an accurate national mapping reference framework and basic mapping. In addition, Ina-CORS can be used to monitor the movement of tectonic plates, conduct geodynamic studies, support atmospheric research, study the ionosphere, and monitor earthquakes and tsunamis [20].

Ina-CORS is part of the Geodetic Control Network, which serves as the realization of the Indonesian Geospatial Reference System (SRGI). The SRGI currently in effect in Indonesia is SRGI 2013. Based on the Regulation of the Geospatial Information Agency (PerBIG) Number 13 of 2021 concerning the Indonesian Geospatial Reference System, the Geodetic Control Network (JKG) is divided into three (3), namely the National Horizontal Control Network (JKHN), the National Vertical Control Network (JKVN), and the National Gravity Control Network (JKGN). JKG is realized using Geodetic Control Points (TKG). Every measurement and mapping activity in Indonesia must use the reference points in the Geodetic Control Network [20].

4. Research Methodology

The data used for deformation observation are GNSS CORS station observations from seven stations. The data were downloaded from the site https://srgi.big.go.id/jkg-active, owned by the Geospatial Information Agency (BIG). The Day of Year (DoY) of GNSS observation data used to calculate deformation is seven days before and after the earthquake day. The earthquake day is DoY 325 in 2022. The locations of the seven stations can be seen in Figure 1. The DoYs used before the earthquake were DoY 297-303. Meanwhile, the DoYs after the quake were DoY 325-331. The distance from the station to the earthquake epicenter varies from 15 to 68 km. More details can be seen in Table 1. GNSS CORS BIG observation data were processed using GAMIT/GLOBK software, with processing carried out using IGS station reference points. In this study, 13 IGS stations were used: ALIC, COCO, CUSV, DARW, DGAR, GUAM, HYDE, IISC, LHAZ, NTUS, PIMO, XMIS, and YARR. The supporting data used were precise ephemeris data and ionosphere data.

Table 1: GNSS CORS stations and distance to epicenter [20]

STA	Latitude	Longitude	Distance (km)
Epicenter	-6.836000	106.997000	0
CJUR	-6.822091	107.138141	15.677
CLDO	-6.767331	106.830302	19.930
CUMI	-7.057161	106.800917	32.676
BAKO	-6.491055	106.848912	41.513
CPWK	-6.551118	107.443059	58.523
CBTU	-6.308319	107.096369	59.381
CLBG	-6.824439	107.615600	68.389

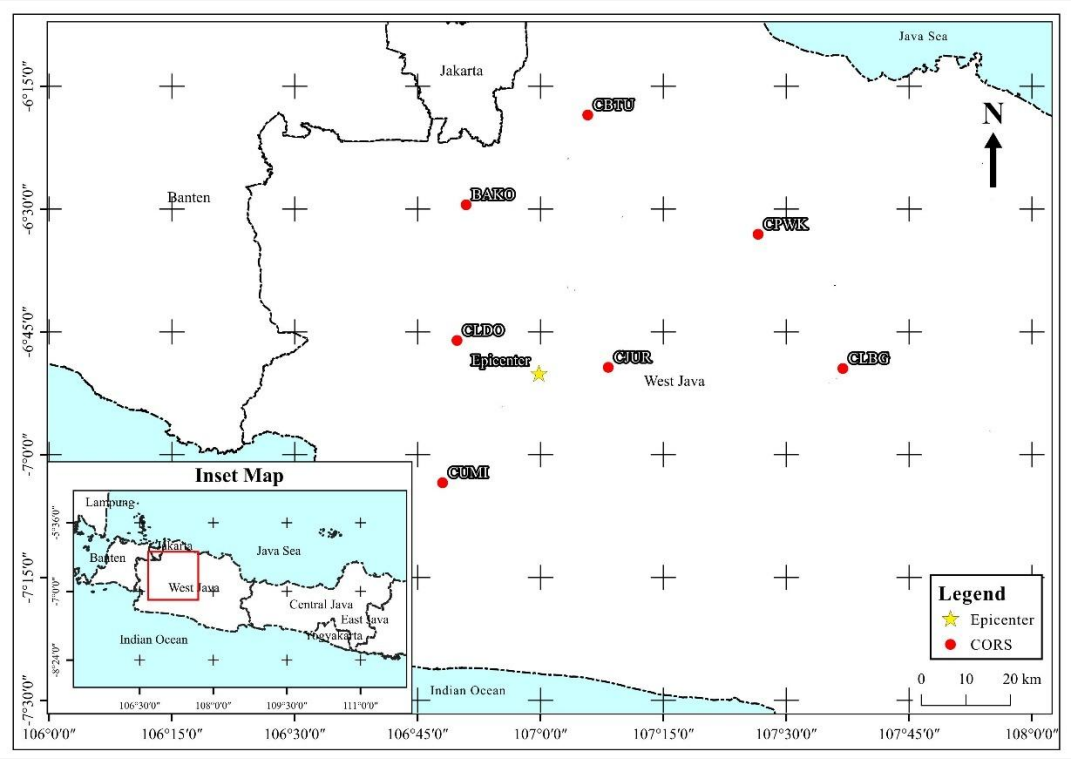

Figure 1: Distribution of GNSS CORS stations [20]

The GAMIT/GLOBK processing results include the geocentric, geodetic, and topocentric coordinates of each GNSS CORS BIG station. GAMIT/GLOBK processing parameters:

1. Elevation Mask: 15^0
2. RINEX Data Time Interval: 30”
3. Precise ephemeris data accessed from http://garner.ucsd.edu/pub/products/
4. Ionex data processed and accessible through https://cddis.nasa.gov/archive/gnss/products/ionex/
5. Ocean wave modeling data (file otl_FES2004.grid) accessed through http://garner.ucsd.edu/pub/gamit/tables/
6. Weather modeling data (files vmf1grd.2022, vmf1grd.2023, and vmf1grd.2024) accessed through http://garner.ucsd.edu/pub/gamit/tables/
7. Atmospheric data (files atmdisp_cm.2022, atmdisp_cm.2023, and atmdisp_cm.2024) accessed through: ftp://everest.mit.edu/pub/GRIDS/

GNSS data quality checks were performed using TEQC (Translating, Editing, and Quality Checking) software, with results showing that the moving average values of MP1 and MP2 were, on average, less than 0.5. Data with moving average values greater than 0.5 were still used due to limitations in data availability. The coordinates from seven days before the earthquake at each station were averaged to become the station's coordinates before the quake. Likewise, the coordinates from seven days after the earthquake became the station's coordinates. The formulas for the average coordinates before and after the earthquake are given in Equations 1 and 2, respectively [21].

$$(n,e,u)^{before} = \frac{1}{N}\sum_{i=1}^{N}\left(n_i^{before}, e_i^{before}, u_i^{before}\right)$$

Equation 1

$$(n,e,u)^{after} = \frac{1}{N}\sum_{i=1}^{N}\left(n_i^{after}, e_i^{after}, u_i^{after}\right)$$

Equation 2

The STA coordinates of the epoch before the earthquake are the STA coordinates of epoch 2012.0 plus the magnitude of deformation from 2012 to the epoch before the quake. While the STA coordinates of epoch after the earthquake are the STA coordinates of epoch 2012.0 plus the magnitude of deformation from 2012 to epoch after the earthquake.

The magnitude of deformation from the 2012 epoch to the epoch before and after the earthquake can be calculated from the deformation model provided in SRGI 2013. Based on the 2013 SRGI model, the magnitude of the displacement velocity in the area around the Cianjur earthquake was 25 mm/year [22]. The difference between the DoY of the data after the earthquake (DoY 325) and before the quake is (DoY 303) is 22 days or 0.06 years, so that the difference between $(dn, de, du)_{after}$ and $(dn, de, du)_{before}$ is 0.06 years times 25 mm/year equal to 1.5 mm. If the value of 1.5 mm is ignored, then $(dn, de, du)_{after} = (dn, de, du)_{before}$. So that the displacement at the observation station $(dn, de, du)_{STA}$ can be determined from Equation 3:

$$(dn, de, du)_{STA} = (n, e, u)^{after} - (n, e, u)^{before}$$

Equation 3

The standard deviation of the average coordinates is the average of the standard deviations of the coordinates of the 7 DoYs. Similarly, the average coordinates after the earthquake are calculated. The standard deviation of the displacement is the average of the standard deviations of the average coordinates before and after the earthquake. The displacement values and standard deviations for each station were statistically tested to determine the significance of the displacement at each station. Then, it was analyzed for accuracy on maps at scales 1:1000, 1:500, and 1:100. The research flow diagram can be seen in the Figure 2.

A t-test was conducted to determine whether the average coordinates before and after the earthquake were the same or different. The difference between the two coordinates represents the horizontal and vertical displacements of the CORS stations. Therefore, the test variables are the horizontal (d_{hor}) and vertical (d_{ver}) displacements for each station. The null hypothesis for this statistical test is that the observation point does not experience a displacement, or that $d_{hor} = 0$ and $d_{ver} = 0$.

The t-value is calculated using the CORS displacement value and the combined standard deviation of the coordinates before and after the earthquake. The number of data points used before and after the quake was seven each, for a total of 14. The combined degrees of freedom value was 12. A limited number of DoYs were utilized to ensure that the calculated deformation was influenced exclusively by the Cianjur earthquake. The t-table at a 95% confidence interval with degrees of freedom = 12 ($t_{12, 0.025}$) is 2.179. Therefore, if the calculated t-value is greater than the t-table value, the point is considered to have displaced or to show a difference between the coordinates before and after the earthquake.

5. Results and Discussion

5.1 Observation Station Coordinates

The average coordinates before and after the earthquake can be seen in Table 2 and Table 3. The coordinates displayed are the topocentric coordinates of northing (n), easting (e), and up-down (u) in the Mercator map projection.

5.2 The Deformation of GNSS CORS

The magnitude of the displacement due to the 2022 Cianjur Earthquake can be seen in Table 4 and Table 5, while the displacement image is in Figure 3. The CORS displacement in Figure 3 is indicated by an arrow line with an error ellipse. In Table 4, the displacement value is expressed in three components: north-south (dn), east-west (de), and vertical (du). A positive value in the dn component indicates a displacement to the north, and a positive value in the de component indicates a displacement to the east; conversely, negative values indicate a displacement to the south or west. At the same time, a positive value in the du component indicates an upward displacement and a negative one indicates a downward displacement.

Table 4 also shows horizontal and vertical deformations. The horizontal displacement (d_{hor}) value is the result of the de and dn displacements. At the same time, the du value is the vertical displacement. The horizontal displacement of the GNSS CORS station ranges from 0.001 m to 0.0445 m or 1 mm to 44.5 mm. The vertical displacement ranges from -0.0038 m to 0.0125 m or -3.8 mm to 12.5 mm. The largest horizontal and vertical displacements are at CJUR Station, which is the closest station to the epicenter. The CJUR Station is being displaced to the southeast and is experiencing an uplift. The magnitudes of horizontal and vertical deformation differ considerably from those calculated using the InSAR method, which reached 120 mm horizontally and 58 mm vertically. The direction of horizontal displacement is consistent, both pointing toward the Southeast. In the InSAR calculations, no uncertainty or standard deviation was reported [18].

Although CJUR and CLDO stations are located at similar distances from the epicenter, their deformation magnitudes differ significantly. Based on the USGS Earthquake Intensity Map, the CJUR area experienced an intensity of VII, or VI based on high-rate GNSS measurements, while CLDO experienced an intensity of V [12] and [15].

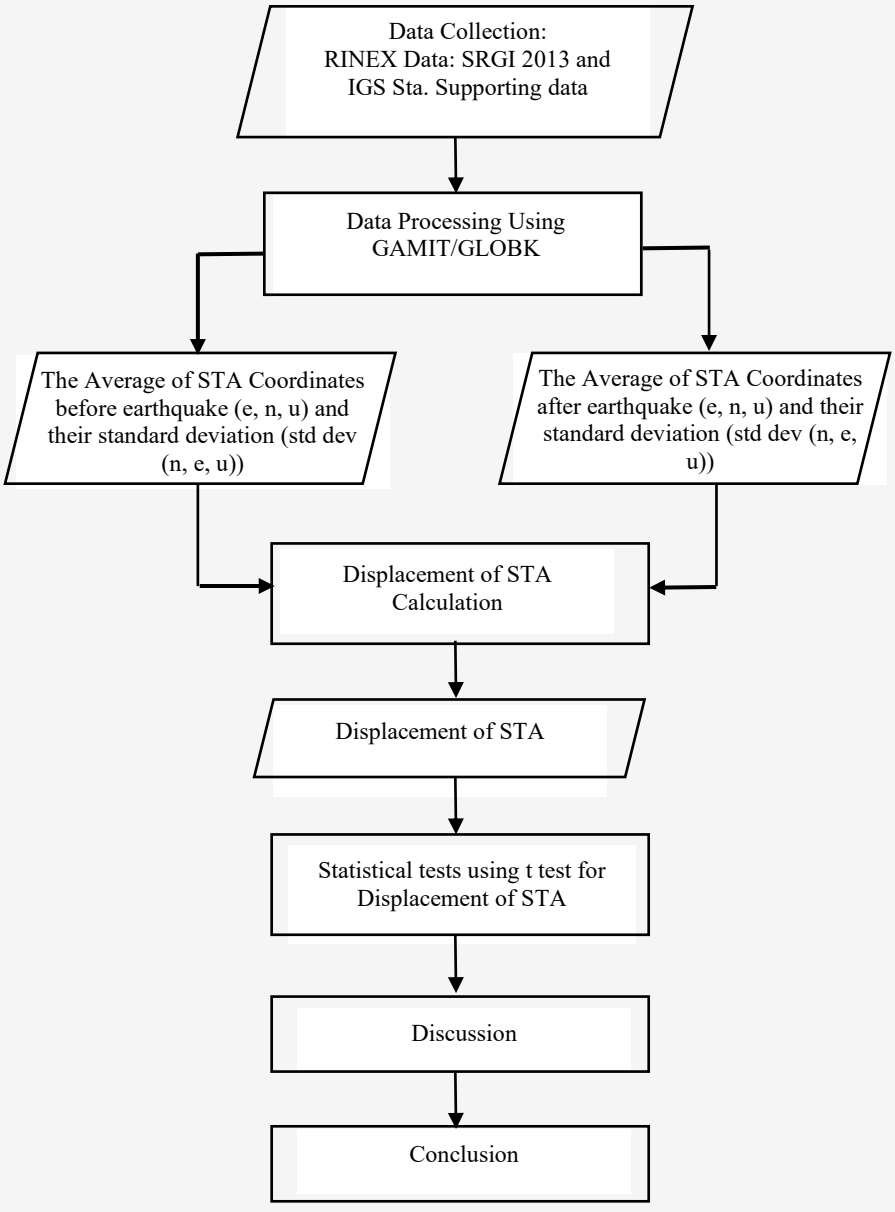

Figure 2: Displacement at GNSS observation station study workflow

Table 2: Average coordinates of GNSS CORS stations before the earthquake

Station	Coordinates (meters)			Standard deviation (meters)		
	n	e	u	n	e	u
CJUR	-759431.747	11842141.173	479.890	0.0017	0.0028	0.0026
CLDO	-753335.903	11809451.794	682.670	0.0054	0.0067	0.0011
CUMI	-785599.673	11798978.494	534.343	0.0037	0.0038	0.0015
BAKO	-722581.022	11818100.115	158.110	0.0018	0.0028	0.0093
CPWK	-729267.136	11882389.667	108.494	0.0035	0.0045	0.0014
CBTU	-702238.928	11849722.953	64.592	0.0024	0.003	0.0019
CLBG	-759693.114	11894844.256	1329.748	0.0026	0.0035	0.0039

Table 3: Average coordinates of GNSS CORS stations after the earthquake

Station	Coordinates (meters)			Standard deviation (meters)		
	n	e	u	n	e	u
CJUR	-759431.766	11842141.213	479.902	0.0013	0.0026	0.0022
CLDO	-753335.904	11809451.794	682.679	0.0066	0.0063	0.0015
CUMI	-785599.675	11798978.492	534.347	0.0029	0.0046	0.0013
BAKO	-722581.023	11818100.114	158.111	0.0016	0.0026	0.0097
CPWK	-729267.138	11882389.667	108.498	0.0029	0.0039	0.0014
CBTU	-702238.931	11849722.954	64.588	0.0028	0.0034	0.0019
CLBG	-759693.116	11894844.258	1329.749	0.0034	0.0039	0.0037

Table 4: The displacement of GNSS CORS

STA	displacement (meters)			
	dn	de	d_{hor}	d_{ver}
CJUR	-0.0187	0.0404	0.0445	0.0125
CLDO	-0.0010	0.0001	0.0010	0.0088
CUMI	-0.0017	0.0004	0.0017	0.0041
BAKO	-0.0010	-0.0013	0.0016	0.0012
CPWK	-0.0011	0.0008	0.0014	0.0041
CBTU	-0.0027	0.0002	0.0027	-0.0038
CLBG	-0.0019	0.0014	0.0024	0.0007

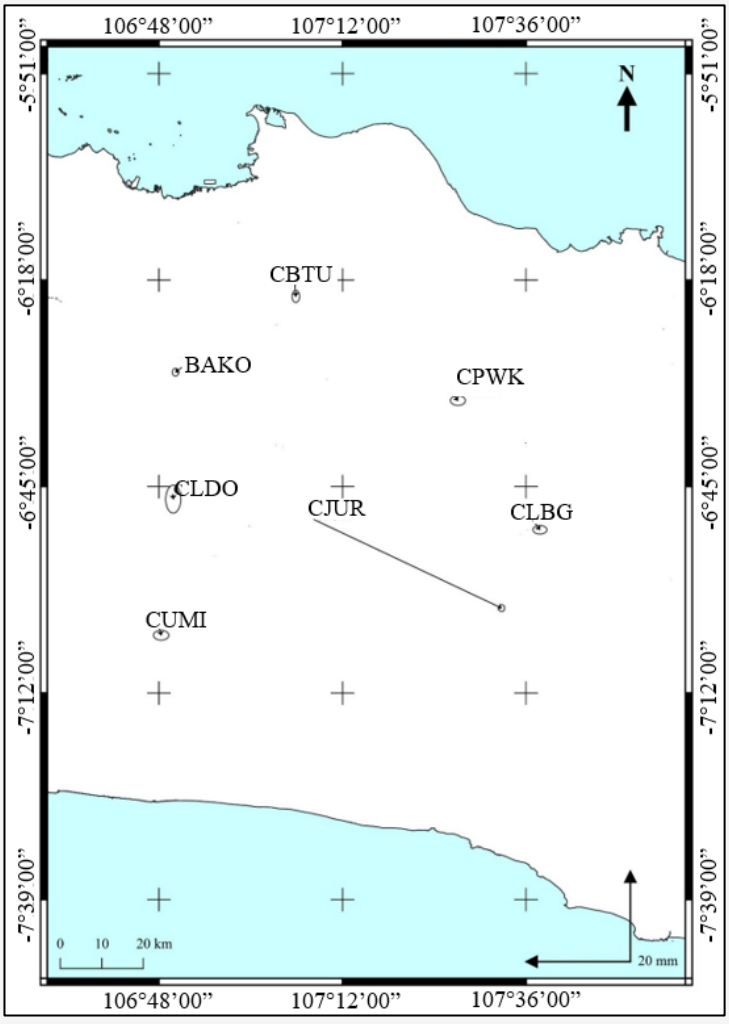

Figure 3: The horizontal displacement of GNSS CORS

The patterns of deformation at CORS stations due to the 2007 Bengkulu earthquake in Indonesia and the 2025 Dapu earthquake in Taiwan are also irregular with respect to distance from the epicenter. In both cases, an inversion was performed on the deformation data. The inversion calculations yielded the slip distribution across the fault plane, revealing its spatial variation [21] and [23]. Therefore, distance from the epicenter is not the primary factor determining the magnitude of deformation or earthquake intensity. One limitation of this study is the limited distribution of CORS points around the earthquake source area. Of the seven CORS points analyzed, only one CJUR experienced significant deformation. Therefore, further analysis of near-field deformation modeling using GNSS CORS data and the least squares inversion method could not be performed. If a deformation model for the earthquake source area could be obtained, surface deformation in that region could be more accurately characterized.

5.3 The Displacements Statistical Test

The results of the displacement significance test are shown in Table 5. It shows that only STA CJUR experienced a significant horizontal displacement of 44.5 mm; the other STAs were considered not to have displacement. As for vertical displacement, five stations showed significant displacement: STA CJUR, CLDO, CUMI, CPWK, and CBTU. Only STA CJUR experienced significant horizontal and vertical displacement.

5.4 The Map Accuracy

Table 6 Shows the accuracy of the large-scale map at 1:1000. 1:500 and 1:100. Horizontal accuracy is calculated at Circular Error 90% (CE90) for Class 1 (0.3 mm x scale number), Class 2 (0.6 mm x scale number) and Class 3 (0.9 mm x scale number). Vertical accuracy is calculated at Linear Error 90% (LE90) for Class 1 (0.5 mm x contour interval), Class 2 (1.5 x class 1 accuracy), and Class 3 (2 x class 1 accuracy) [24]. The horizontal displacement of STA CJUR is 44.5 mm. As seen in Table 6, the deformation of STA CJUR affects the 1:100 class 1 scale map, which has an accuracy tolerance of 20 mm. Meanwhile, the vertical displacements at the five stations that showed significant displacement, with a maximum of 12.5 mm at STA CJUR, did not affect the 1:100 class 1 scale map, which has an accuracy tolerance of 20 mm.

The measurement and calculation of point coordinates referencing STA CJUR use reference coordinates with the 2012 epoch and the SRGI 2013 deformation model. STA CJUR is one of the benchmarks in the SRGI 2013 reference frame used as a reference for measurement and mapping activities. The horizontal control network accuracy for the first, second, and third orders in Australia and New Zealand are 5 mm, 12 mm, and 25 mm, respectively [25]. Meanwhile, according to the Draft Indonesian National Standard for Geodetic Control Networks, the horizontal control network accuracy for the zero, first, and second orders is 5 mm, 20 mm, and 45 mm, respectively [26]. STA CJUR, as a GNSS CORS, is a zero-order control point. Therefore, given the significant changes in STA CJUR coordinates due to the coseismic deformation caused by the Cianjur Earthquake on November 22, 2022, the reference coordinates of STA CJUR need to be redefined.

Table 5: The significance of horizontal and vertical displacement of GNSS CORS

STA	t_{hor}	t_{ver}	The STA is displaced horizontally	The STA is displaced vertically
CJUR	32.854	9.71	Yes	Yes
CLDO	0.308	12.52	No	Yes
CUMI	0.917	5.46	No	Yes
BAKO	1.227	0.24	No	No
CPWK	0.751	5.48	No	Yes
CBTU	1.929	3.74	No	Yes
CLBG	1.391	0.34	No	No

Table 6: The base map geometric accuracy (unit in mm)

Map Scale	Contour Interval	1st Class		2nd Class		3rd Class	
		Horizontal	Vertical	Horizontal	Vertical	Horizontal	Vertical
1:1000	400	300	200	600	300	900	400
1:500	200	150	100	300	225	450	200
1:100	40	30	20	60	30	90	40

Redefining the STA CJUR coordinates with an epoch after the Cianjur earthquake will allow points measured using the STA CJUR reference to accommodate the deformation caused by the earthquake. Many measurement and mapping activities require a scale of 1:100 or larger. According to Equation 4, the STA coordinates after the earthquake are derived from the STA coordinates at epoch 2012, the deformation of the STA from 2012 to the DoY after the earthquake based on the deformation model, and the displacement of the STA due to the earthquake. The current deformation model for the semi-dynamic datum does not yet account for earthquake-induced deformation. Therefore, to obtain accurate STA coordinates for the reference frame, earthquake-induced deformation values must be incorporated.

The deformation caused by the 2022 Cianjur earthquake did not significantly impact the 1:1000-scale maps used in Indonesia for cadastral mapping, the 1:5000-scale maps for village maps, or smaller-scale maps. However, measurement and mapping activities consist of control point measurement at an order below the SRGI 2013 reference frame and detail point measurement and mapping according to the thematic requirements of the map. These control point measurement and densification activities utilize SRGI 2013 reference frame points as references, including STA CJUR. The required precision for these control point measurements is 20 mm for Order 1 and 45 mm for Order 2. Control point measurement activities of an order below the SRGI 2013 reference frame are used for cadastral measurement and mapping at a scale of 1:1000. Cadastral measurement and mapping often employ new control point references measured against the SRGI 2013 reference frame, as the mapping areas are frequently located far from the existing SRGI 2013 reference frame control points. Consequently, a displacement of 44.5 mm at STA CJUR can affect control point measurement activities used in thematic mapping.

6. Conclusion

The 2022 Cianjur earthquake (Mw 5.6) caused significant deformation at a single CORS point in the SRGI 2013 reference frame. It was among the destructive earthquakes that have occurred in Indonesia since 2013, resulting in hundreds of fatalities. Several other destructive earthquakes with significant casualties occurring in Indonesia since 2013 include the 2016 Aceh earthquake, the 2018 Lombok earthquake, and the 2018 Palu earthquake, all of which had magnitudes exceeding 6.0. Given that the Cianjur earthquake had a magnitude of only 5.6 yet caused significant deformation at a single CORS point in the SRGI 2013 reference frame, greater attention should be paid to the influence of earthquake-induced deformation on the CORS station network of the SRGI 2013 reference frame, particularly given Indonesia's exceptionally high seismicity. The Mw 5.6 Cianjur earthquake caused significant deformation at a single CORS point, detectable at map scales as large as 1:100. Although this deformation is not significant on maps at scales of 1:1,000 or smaller, it can affect lower-order control point measurements used for 1:1,000-scale mapping.

The SRGI 2013 deformation model does not yet account for earthquake-induced deformation. Therefore, deformation analysis at CORS stations around the earthquake epicenter is necessary to determine the impact of coseismic deformation on the SRGI 2013 reference frame. Redefining the CORS station coordinates using updated epochs or incorporating earthquake-induced deformation into the deformation model are both viable approaches. The sparse distribution of CORS stations around the earthquake source area precludes further analysis aimed at deriving a near-field deformation model. Such a model is essential for more accurately characterizing surface deformation in the source area. Therefore, areas around earthquake sources should be prioritized for the development of new CORS stations within the SRGI reference framework.

Acknowledgements

Thanks to the Indonesian Geospatial Information Agency for the 2013 SRGI GNSS CORS data, which can be downloaded for free at https://srgi.big.go.id/rinex/v1/download-file-box.

References

[1] Jufriansah, A., Pramudya, Y., Khusnani, A. and Saputra, S., (2021). Analysis of Earthquake Activity in Indonesia by Clustering Method. *Journal of Physics: Theories and Applications*, Vol. 5(2). https://doi.org/10.20961/jphystheor-appl.v5i2.59133.

[2] SRGI Tunggal untuk One Map Policy [Single SRGI for One Map Policy]. Badan Informasi Geospasial. Available: https://big.go.id/news/2014/04/25/srgi-tunggal-untuk-one-map-policy. [Accessed: Dec. 20, 2024].

[3] Susilo, Abidin, H. Z., Meilano, I., Sapiie, B., Gunawan, E., Wijarnto, A. B. and Efendi, J., (2017). Preliminary Co-seismic Deformation Model for Indonesia Geospatial Reference System 2013. *AIP Publishing LLC*, Vol. 1857. https://doi.org/10.1063/1.4987073.

[4] Li, C. K., Ching, K. E. and Chen, K. H., (2019). The Ongoing Modernization of the Taiwan Semi-Dynamic Datum Based on the Surface Horizontal Deformation Model using GNSS Data from 2000 to 2016. *Journal of Geodesy*, Vol. 93(9); 1543–1558. https://doi.org/10.1007/s00190-019-01267-5.

[5] Dewanto, B. G., Wijaya, C. and Priadi, R., (2025). The Palu-Koro Fault Behaviour Monitoring Associated with the 2018 Palu Earthquake Based on the Multi-Temporal PlanetScope and Landsat 8 Satellite Images. *Remote Sensing Applications: Society and Environment*, Vol. 37. https://doi.org/10.1016/j.rsase.2024.101397.

[6] Nurdin, N., Pujiastuti, D. and Marzuki, M., (2024). Seismic Deformation of the Palu Koro Fault Due to the 2018 Palu Earthquake Using Global Navigation Satellite System Data. *AIP Conference Proceedings,* Vol. 2891. https://doi.org/ 10.1063/5.0201192.

[7] Nurtyawan R. and Yulanda, M. F., (2020). Lombok Earthquakes Using DInSAR Techniques Based on Sentinel 1a Data (Case Study: Lombok, West Nusa Tenggara). *IOP Conference Series: Earth and Environmental Science*, Vol. 500. https://doi.org/10.1088/1755-1315/500/1/012 065.

[8] Awaluddin, M., Yuwono, B. D. and Puspita, Y. A., (2016). Slip Distribution of the 2010 Mentawai Earthquake from GPS Observation Using the Least Squares Inversion Method. *AIP Conference Proceedings,* Vol. 1730. https://doi.org/10.1063/1.4947392.

[9] Djenaliev, A., Kada, M., Chymyrov, A., Hellwich, O., Bairamov, E. and Muraliev, A., (2022). Investigation of Earthquake Deformation Detectability Using Sentinel-1 Interferometric Data. *International Journal of Geoinformatics*, Vol. 18(6); 81–96. https://doi.org/10.52939/ijg.v18i6.2453.

[10] Dong, Z., Meng, G., Xu, Y., Wu, W., Wei, C., Yang, Y. and Wang, Y., (2025). Coseismic Deformation and Kinematic Rupture Process of the 2023 Türkiye M W7.8–7.5 Earthquake Doublet Deduced from High-Rate GNSS Observations. *Geophysical Journal International*, Vol. 240(3); 1363–1374. https://doi.org/10.1093/gji/ggae445.

[11] Fazilova, D., Makhmudov, M. and Magdiev, K., (2023). Analysis of Crustal Movements in the Angren-Almalyk Mining Industrial Area Using GNSS Data. *International Journal of Geoinformatics*, Vol. 19(11); 12–19. https://doi.org/10.52939/ijg.v19i11.2915

[12] M 5.6 - 11 km NE of Sukabumi, Indonesia Shake Map. The U.S. Geological Survey. Available: https://earthquake.usgs.gov/earthquakes/eventpage/us7000ir9t/shakemap/intensity [Accessed: Jan. 15, 2025].

[13] Peta Bahaya Gempabumi Cianjur (dengan Sumber Gempa Patahan Cugenang) [Cianjur Earthquake Hazard Map (with Cugenang Fault Earthquake Source)]. Badan Meteorologi, Klimatologi dan Geofisika. Available: https://www.bmkg.go.id/siaran-pers/peta-bahaya-gempabumi-cianjur-dengan-sumber-gempa-patahan-cugenang. [Accessed: Jan. 20, 2025]

[14] Supendi, P., Winder, T., Rawlinson, N., Bacon, C. A., Palgunadi, K. H., Simanjuntak, A. V. H., Kurniawan, A., Widiyantoro, S., Nugraha, A. D., Ash Shiddiqi, H., Adi, S. P., Karnawati, D., Marliyani, G. I., Imran, I. and Jatnika, J., (2023). A Conjugate Fault Revealed by the Destructive Mw 5.6 (November 21, 2022) Cianjur Earthquake, West Java, Indonesia. *Journal of Asian Earth Sciences*, Vol 257. https://doi.org/10.1016/j.jseaes.2023.105830.

[15] Meilano, I., Susilo and Wibowo, S. T., (2023). Peak Ground Velocity (PGV) Estimation of Mw 5.6 Cianjur Earthquake November 11, 2022 Using Global Positioning System (GPS). *IOP Conference Series: Earth and Environmental Science*, Vol. 1245. https://doi.org/10.1088/1755-1315/1245/1/012030.

[16] Zulfakriza, Z., Nugraha, A. D., Heryandoko, N., Ry, R. V., Muttaqy, F., Andika, A., Azhari, M. F., Putra, A. S., Palgunadi, K. H., Cummins, P. R., Supendi, P., Lesmana, A., Sahara, D. P. and Puspito, N. T., (2024). Seismic Source Analysis of the Destructive Earthquake November 21, 2022, Mw 5.6 Cianjur (Indonesia) from Relocated Aftershock. *Scientific Reports,* Vol. 14. https://doi.org/10.1038/s41598-024-60408-9.

[17] Prayogo, M. A., (2023). Analysis of Land Cover and Building Damage Due to the 21st November 2022 Cianjur Earthquake using Sentinel-2. *IOP Conference Series: Earth and Environmental Science*, Vol. 1276(1). https://doi.org/10.1088/1755-1315/1276/1/012037.

[18] Hanif, M. and Tongleamnak, S., (2024). The Quantifying Crustal Deformation Caused by the Cianjur Tectonic Earthquakes Magnitude 5.6 through InSAR and GNSS Technology. *Bulletin of Earth Sciences of Thailand*, Vol. 16(1). https://ph01.tci-thaijo.org/index.php/bestjournal/article/view/256321.

[19] Hadmoko, D. S., Wibowo, S. B. and Sianipar, D. S. J., (2024). Co-Seismic Deformation and Related Hazards Associated with the 2022 Mw 5.6 Cianjur Earthquake in West Java, Indonesia: Insights from Combined Seismological Analysis, Dinsar, and Geomorphological Investigations. *Geoenvironmental Disasters*, Vol. 11. https://doi.org/10.1186/s40677-024-00277-6.

[20] Jaring Kontrol Geodesi [Geodetic Control Network]. Badan Informasi Geospasial. [Online] Available: https://srgi.big.go.id/page/jaring-kontrol-geodesi. [Accessed: Dec. 20, 2024].

[21] Awaluddin, M., Meilano, I. and Widiyantoro, S., (2012). Estimation of Slip Distribution of the 2007 Bengkulu Earthquake from GPS Observations Using the Least-Squares Inversion Method. *ITB Journal of Engineering Science*, Vol. 44(2); 187–206. https://doi.org/10.5614/ITBJ.ENG.SCI.2012.44.2.6

[22] Model Deformasi [Deformation Model]. Badan Informasi Geospasial. [Online] Available: https://srgi.big.go.id/deformasi-active [Accessed: Sep. 28, 2025].

[23] Lee, Z., Chuang, R. Y., Wang, I. T., Chen, L., Chang, W. L., Chiu, C. Y., Ching, K. E., Guo, S. W. and Chen, C. L., (2025). Fast Report: Surface Deformation Associated with the 2025 Dapu Earthquake. *Terrestrial, Atmospheric and Oceanic Sciences*, Vol. 36(11). https://doi.org/10.1007/s44195-025-00090-0.

[24] Pedoman Teknis Ketelitian Peta Dasar Badan Informasi Geospasial [Technical Guidelines for the Accuracy of Geospatial Information Agency Base Maps]. (2018). Peraturan Badan Informasi Geospasial Nomor 6 tahun 2018 tentang Perubahan atas Peraturan Kepala Badan Informasi Geospasial Nomor 15 tahun 2014 [Geospatial Information Agency Regulation Number 6 of 2018 concerning Amendments to the Regulation of the Head of the Geospatial Information Agency Number 15 of 2014].

[25] Dąbrowski, J., (2014). Accuracy Standards of Tying the Horizontal and Vertical Control Network to the National Geodetic Control Network. *Geomatics and Environmental Engineering*, Vol. 8(3). https://doi.org/10.7494/geom.2014.8.3.41.

[26] Jaring Kontrol Geodesi [Geodesic Control Network]. (2024). Badan Standar Nasional: SNI 9217:2024.